Crystal Structure of Bovine Pancreatic Phospholipase A2 Covalently Inhibited by p-Bromo-phenacyl-bromide

Renetseder, Roland; Dijkstra, Bauke W.; Huizinga, Kees; Kalk, Kor H.; Drenth, Jan

Published in:
Journal of Molecular Biology

DOI:
10.1016/0022-2836(88)90342-7

Publication date:
1988

J. Mol. Biol. (1988) 200, 181–188

Crystal Structure of Bovine Pancreatic Phospholipase A_2 Covalently Inhibited by *p*-Bromo-phenacyl-bromide

Roland Renetseder†, Bauke W. Dijkstra‡, Kees Huizinga Kor H. Kalk and Jan Drenth

Laboratory of Chemical Physics
University of Groningen, Nijenborgh 16
9747 AG Groningen, The Netherlands

(Received 19 August 1987, and in revised form 23 October 1987)

Bovine pancreatic phospholipase A_2 covalently inhibited by *p*-bromo-phenacyl-bromide was crystallized from 50% (v/v) 2-methyl-2,4-pentanediol. The space group was $P3_121$ with cell dimensions $a = b = 46{\cdot}73$ Å and $c = 102{\cdot}5$ Å (1 Å = 0·1 nm). Diffraction data were collected by oscillation photography from one single crystal of dimensions 0·2 mm × 0·2 mm × 0·2 mm. The crystal structure was determined to a resolution of 2·5 Å by crystallographic refinement of a starting model, which consisted of native bovine pancreatic phospholipase A_2 positioned and oriented in the $P3_121$ cell as in the bovine pro-phospholipase A_2. The crystallographic *R*-factor decreased from 0·378 to 0·197 after 70 refinement cycles. For the greater part the three-dimensional structure was very similar to that of native phospholipase. The inhibitor group shows up clearly. However, as in solution, there is no calcium ion bound any more in the active site, and this causes a significant conformational change in the loop from residue 59 to 73. This loop is remote from the calcium binding site. Interestingly, this is the same loop that also shows different conformations in other phospholipase A_2 molecules.

The inhibitor molecule has hydrophobic interactions with Phe5 and Cys45. Rational design of specific and potent inhibitors of phospholipase A_2 catalysis is discussed on the basis of the present three-dimensional structure.

1. Introduction

Phospholipase A_2 catalyses the hydrolysis of the 2-acylester bond of 3-*sn*-glycerophospholipids. The enzyme occurs both extracellularly and within cells. Extracellular phospholipases A_2 have been isolated in abundance from mammalian pancreas and from snake and bee venoms (for reviews, see Verheij *et al.*, 1981; Volwerk & de Haas, 1982; Dennis, 1983). They need calcium ions for their activity (Pieterson *et al.*, 1974*a*; Wells, 1973) and can be inactivated by *p*-bromo-phenacyl-bromide (Volwerk *et al.*, 1974; Halpert *et al.*, 1976). The pancreatic phospholipase A_2 is synthesized as a pro-enzyme. Upon secretion into the gastro-intestinal tract this pro-enzyme is activated by trypsin, which cleaves off the seven N-terminal amino acid residues. The catalytic properties of precursor and enzyme, with respect to monomeric substrates, are quite similar. However, when substrate is present as an aggregate, such as micelles, there is a large increase in enzymatic activity of the mature enzyme, but not of its zymogen (Pieterson *et al.*, 1974*b*). Three-dimensional structures have been determined by X-ray crystallography for phospholipases A_2 from bovine pancreas (Dijkstra *et al.*, 1981*a*), porcine pancreas (Dijkstra *et al.*, 1983*a*) and *Crotalus atrox* venom (Brunie *et al.*, 1985). In addition, the three-dimensional structure of bovine pancreatic pro-phospholipase A_2 is known (Dijkstra *et al.*, 1982). The extracellular phospholipases A_2 show a high degree of sequence homology and also their three-dimensional structures are very similar (Renetseder *et al.*, 1985).

The intracellular phospholipases on the other hand are far less easy to isolate and purify, because they occur in minimal amounts and they are often bound to membranes (for a review, see van den Bosch, 1980). Like the extracellular phospholipases they have been shown to be calcium dependent, and, in one case at least, to be inactivated by *p*-bromo-phenacyl-bromide in the same manner as

† Present address: Hoffmann-La Roche, CH-4002 Basel, Switzerland.

‡ Author to whom all correspondence should be sent.

0022-2836/88/050181-08 $03.00/0

the extracellular ones (de Winter *et al.*, 1982). These intracellular phospholipases A_2 have been implicated to play a role in a variety of physiologically important cellular responses, such as inflammation and blood platelet aggregation. These processes appear to be initiated by the release of arachidonic acid from cell membranes due to the stimulation of intracellular phospholipases A_2 (Lewis & Austen, 1981). Recently, a phospholipase A_2 has been isolated from sterile inflammatory peritoneal exudates, which shows, in its first 39 N-terminal amino acid residues, an appreciable sequence homology with pancreatic and snake venom phospholipases A_2 (Forst *et al.*, 1986; the remainder of the sequence was not published). This indicates that there exists similarity between the pancreatic and snake venom phospholipases A_2 and at least one of the intracellular ones.

Because of the crucial role of intracellular phospholipases A_2, there is a great interest in specific inhibitors for phospholipase A_2 in order to prevent or suppress the consequences of phospholipase A_2 action in certain pathological cases of chronic inflammation, such as rheumatoid arthritis and asthma. To this end a clear understanding of the interaction of phospholipases A_2 with substrates and inhibitors is required. As a first step towards this understanding we determined the X-ray structure of a pancreatic phospholipase A_2 covalently inhibited by *p*-bromo-phenacyl-bromide. This allowed us to define part of the hydrophobic binding site for monomeric phospholipids.

2. Materials and Methods

(a) *Crystallization*

Bovine pancreatic phospholipase A_2, covalently modified with *p*-bromo-phenacyl-bromide (Volwerk *et al.*, 1974), was generously provided by Professor de Haas and co-workers (Utrecht). The protein was set to crystallize under standard conditions for bovine phospholipase A_2: freeze dried protein was dissolved in 50 mM-Tris·HCl (pH 7·2), 5 mM-$CaCl_2$ to a concentration of 10 to 15 mg/ml ($\approx$1 mM). Portions (50 μl) of this solution were frozen in small glass tubes at -20°C. 2-Methyl-2,4-pentanediol (Fluka) (50 μl) was layered on top of the frozen solution and the tubes were set aside for crystallization at room temperature. Tiny crystals grew after several months. The present study was undertaken with one crystal (0·2 mm × 0·2 mm × 0·2 mm) taken from these experiments after about 6 years. The space group is $P3_121$ with cell dimensions $a = b = 46{\cdot}73$ Å, $c = 102{\cdot}5$ Å (1 Å = 0·1 nm).

(b) *Data collection*

A 3-dimensional X-ray diffraction data set was collected on an Enraf-Nonius rotation camera (Arndt & Wonacott, 1977) with graphite monochromatized CuKα radiation from an Elliott GX-20 rotating anode generator. The crystal-to-film distance was 75 mm. The crystal was rotated about the c^*-axis with a total scan range of 0·0° to 60·2°, corresponding to roughly 2 asymmetric units of reciprocal space for space group $P3_121$. Due to the lack of suitable crystals, no cusp data were collected. CEA Reflex 25 film (CEA Verken, Strängnäss, Sweden) was used in packs of 2 films/exposure for the registration of the intensities. Films were digitized on a SCANDIG rotating drum scanner in a 50 μm × 50 μm raster and then averaged to a 100 μm × 100 μm raster. Film data were evaluated to a maximum resolution of 2·5 Å by a modified version of the program of Schwager *et al.* (1973). Raw data were corrected for paper and film absorption and skew incidence. Structure factor amplitudes derived from the fully recorded reflections of all packs were used for the calculation of relative scale and temperature factors by an extension of the method of Hamilton *et al.* (1965). Individual reflections contributed with a weight of $1/\sigma^2$, using $\sigma(F)$ from the film evaluation program. Scale and temperature factors were applied to all data and partially recorded reflections from successive packs were combined. Finally, multiple observations of equivalent reflections were averaged and actual effective standard deviations (σ_{eff}) calculated from the deviations from the weighted mean, again using $1/\sigma^2$ as weighting factors:

$$\bar{F} = \frac{\sum_i \frac{1}{\sigma_i^2} F_i}{\sum_i \frac{1}{\sigma_i^2}}, \quad \sigma_{\text{eff}} = \left(\frac{\sum_i \frac{1}{\sigma_i^2} (F_i - \bar{F}_w)^2}{\sum_i \frac{1}{\sigma_i^2}} \right)^{\frac{1}{2}}.$$

Data deviating more than $2\sigma_{\text{eff}}$ from the weighted mean were rejected and the corresponding values recalculated.

(c) *Crystallographic refinement*

Two types of refinement procedure were used alternatingly: a $P3_121$-specific version of the fast Fourier transform refinement of Agarwal (1978) in combination with a separate regularization procedure described by Dodson *et al.* (1976), and the well-known restrained least-squares refinement program of Hendrickson and Konnert (Hendrickson, 1985) with a $P3_121$-specific routine for the calculation of structure factors and derivatives. Each of these procedures has its advantages and drawbacks. The fast Fourier transform refinement (FFTREF) is very easy to use and computationally a very fast free atom refinement program, which in combination with intermittent regularization of the structure provides a large radius of convergence. But with limited diffraction data as in this case (2·5 Å resolution) and a regularization program restraining only bond lengths, angles and planes, this procedure might easily result in a model with rather poor geometry, especially with respect to van der Waals' distances and chiral centres. The restrained least-squares procedure (PROLSQ), on the other hand, is computationally much slower but offers a greater variety and flexibility with respect to geometrical restraints. Therefore, this program can very well be used to improve the geometry of a model refined with FFTREF, while maintaining a reasonable fit between the observed and calculated diffraction data.

The refinement proceeded in several rounds. When a series of refinement cycles had apparently converged as judged by the changes in *R*-factor and shifts, the model was inspected in $F_o - F_c$ and $2F_o - F_c$ maps. Coefficients for the Fourier maps were weighted according to Sim (1959, 1960) as $m(F_o - F_c)$ and $m(2F_o - F_c)$. The XRAY-System (Stewart, 1976) was used for calculating the maps on an arbitrary scale and for searching peaks in the $F_o - F_c$ maps. The highest peaks were carefully analysed and suitable ones included in the model as solvent molecules. Adjustments of the model were made on our E&S PS 11

graphics display system using the program GUIDE (Brandenburg *et al.*, 1981). The refinement was terminated when an acceptable compromise between the geometry of the model and the crystallographic R-factor had been reached and the F_o-F_c and $2F_o-F_c$ maps provided no further clues for improvement of the model.

(d) *Comparison of atomic models*

Superposition of atomic co-ordinate models was performed using the method of Rao & Rossmann (1973), or the method of Kabsch (1976). Both methods gave identical results.

3. Results

(a) *Data collection and processing*

The relatively small cell dimensions perpendicular to the rotation axis allowed for rather large scan angles of 2·4° to 4·0° per film pack. In total, 20 film packs were exposed in the scan range 0 to 60·2°. Table 1 gives a summary of the results of processing the data. The overall completeness of the data set is 75·1% to 2·5 Å resolution. It should be taken into account, that the data were recorded by rotation about one axis only, and that no cusp data were collected.

(b) *Structure determination and refinement*

The cell dimensions of this crystal were very similar to those of bovine pancreatic pro-phospholipase A_2 (Dijkstra *et al.*, 1982) (for a comparison of the two crystal forms see Table 2); also the diffraction pattern was similar to that of the pro-phospholipase A_2 ($R = 0{\cdot}27$; see Table 2). Because part of the pro-phospholipase A_2 structure is disordered, we used as the starting model for the refinement the structure of the refined bovine phospholipase A_2 (Dijkstra *et al.*, 1981*a*) without solvent, positioned as in the bovine pro-phospholipase A_2 crystals (Dijkstra *et al.*, 1982). The starting crystallographic R-factor for this model was 0·378. The positioning was refined by a "manual" rigid-body R-factor search, which resulted in a slight improvement of the R index to 0·364. The corresponding Sim-weighted $2F_o-F_c$ map was clear and unambiguous for the greater part. However, the region of residues 63 to 68 was ill defined, as were the side-chains of residues 31, 34 and 113 to 115. Moreover, the covalently bound inhibitor, which we had hoped to see linked to the active site His48, showed up only very weakly and was not clearly interpretable. A comparable observation was made in the rather noisy F_o-F_c map, where density at a level of about 2σ above average was found near the expected location of the inhibitor, but this density was not readily interpretable either. Therefore, we decided to refine the initial model, leaving out, in the first round, the unclear regions as well as the side-chain of His48 and the Ca ion. In the maps calculated after this

Table 2

Comparison of crystals of bovine pancreatic pro-phospholipase A_2 and p-*bromo-phenacyl-bromide-inactivated phospholipase A_2*

	Space group	Cell dimensions (Å) $a=b$	c
Pro-phospholipase A_2	$P3_121$	46·95	102·0
p-Bromophenacyl bromide inactivated phospholipase A_2	$P3_121$	46·73	102·5
Agreement R-factor†	0·27		

† $R = \dfrac{\sum_{hkl} ||F_1|-|F_2||}{\sum_{hkl} |F_1|}$,

in which $|F_1|$ are the observed structure factor amplitudes for bovine pro-phospholipase and $|F_2|$ are those for *p*-bromo-phenacyl-bromide-inactivated phospholipase A_2, scaled on F_1. Resolution 2·5 Å.

Table 1

Results of data reduction

	Number of observations	R_{sym}†	N_{sym}†	Number of unique reflections
A. *Summary of film data processing*				
Fulls	8234	0·055	7157	3509
Combined partials	1643	0·075	534	
Total	9877	0·063	8808	3718

B. *Completeness of data*

Resolution (Å)	100·0	7·07	5·00	4·08	3·54	3·16	2·89	2·67	2·50
Completeness (%) (shell)	91·4	91·4	93·3	90·3	83·0	74·9	59·9	48·8	
Completeness (%) (sphere)	91·4	91·4	92·2	91·5	89·2	85·9	80·7	75·1	

† $R_{sym} = \dfrac{\sum_{hkl}\sum_i |F_{i,hkl}-\overline{F_{hkl}}|}{\sum_{hkl}\sum_i |F_{hkl}|}$;

N_{sym} is the number of observations over which the summation for the R_{sym} calculation is done.

first round, density for the omitted side-chain of His48 showed up clearly, as well as density for residues 31, 34 and 113 to 115. In contrast, there was no density for the Ca ion. This was to be expected because the modified enzyme in solution does not bind Ca^{2+} any more (Volwerk *et al.*, 1974). Extending from the His48 side-chain at the $N^{\delta}1$ atom, density was observed at a level of 2σ above average in the F_o-F_c and $2F_o-F_c$ maps, which could now easily be interpreted as the modifying group. The density for the loop comprising residues 63 to 67 was still ill defined after this refinement cycle. Although during the refinement several different interpretations for this loop were tried, none of them gave a satisfactory result: the density for this loop remained low and discontinuous.

A total of 70 refinement cycles was performed and 65 water molecules were included in the model. The weighting scheme for the final restrained least-squares refinement cycles and some characteristic values of the final model are given in Table 3. The final *R*-factor is 19·7% for all observed reflections between 6·0 and 2·5 Å resolution. The overall r.m.s.† error in the co-ordinates has been estimated to be about 0·30 Å from a σ_A-plot (Read, 1986), which is in good agreement with other structures refined at a similar resolution (see e.g. Deisenhofer, 1981), for which the r.m.s. error for well-defined atoms was estimated to be 0·25 to 0·30 Å.

(c) *The three-dimensional structure*

Figure 1 shows a comparison of the C^{α}-atom positions in the native and inhibited phospholipase A_2. The greater part of the structure is very similar, including the active site. However, the calcium binding loop (residues 28 to 33) and the loop from residue 59 to 73 show a different conformation (see below). Also some small differences occur in side-chain conformations at the surface of the molecule. Most of these side-chains are not very well defined in either the native or the present structure. Superposition of the C^{α} atoms of native and inhibited phospholipase A_2 results in an r.m.s. co-ordinate difference of 0·86 Å for all 123 C^{α} atoms. Excluding the C^{α} atoms of residues 30 to 33 and 59 to 73 reduces this r.m.s. difference to 0·49 Å.

Table 3

Summary of input parameters and results obtained with the restrained least-squares refinement procedure (after final refinement cycle)

	Input standard deviation	r.m.s. deviation from standard value
1–2 distances (Å)	0·020	0·011
1–3 distances (Å)	0·030	0·034
1–4 distances (Å)	0·050	0·036
Plane distances (Å)	0·020	0·013
Chiral volumes (Å^3)	0·150	0·210
Single torsion contacts (Å)	0·500	0·211
Multiple torsion contacts (Å)	0·500	0·330
Possible H-bonds (Å)	0·500	0·242
S–S bonds (Å)	0·020	0·005
Temperature factors:		
Main-chain bond (Å^2)	2·000	5·92
Main-chain angle (Å^2)	3·000	6·67
Side-chain bond (Å^2)	3·000	9·62
Side-chain angle (Å^2)	4·000	11·12
Structure factors		67·25

p-Bromo-phenacyl-bromide binds covalently to the active site residue His48 (Volwerk *et al.*, 1974). Figure 2 shows the electron density for the inhibitor in the active site. The conformation of the His48 residue is identical with that in the native enzyme. The aromatic group of the inhibitor makes hydrophobic interactions with the side-chains of Phe5, Tyr69 and Cys45 (see Fig. 3). Somewhat further away are the main-chain atoms of Gly30. The oxygen atom of the phenacyl group points in the direction of the C^{α} and C^{β} atoms of Cys45, but, surprisingly, does not make any hydrogen bonds with polar protein atoms or solvent. Thus, apart from the covalent link to the $N^{\delta}1$ atom of His48,

† Abbreviation used: r.m.s., root mean square.

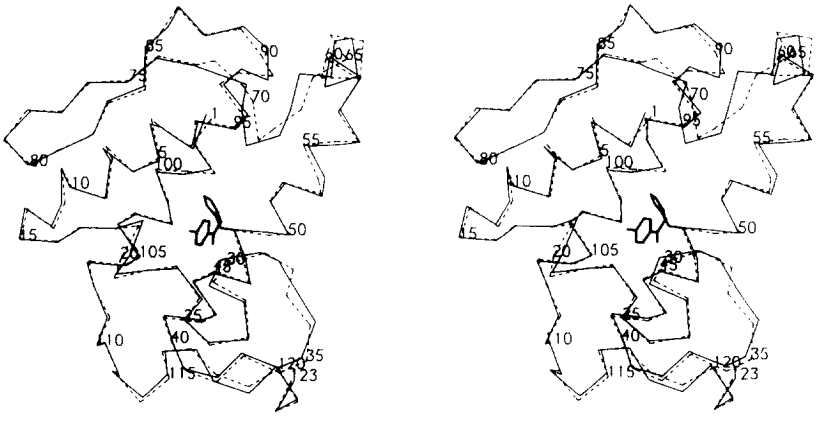

Figure 1. Stereo diagram of the superposition of C^{α} atoms of native and inhibited bovine phospholipase A_2. The native enzyme is indicated by broken lines. Residues 64 to 67 are not well defined in the refined structure of the *p*-bromo-phenacyl-bromide-inhibited enzyme.

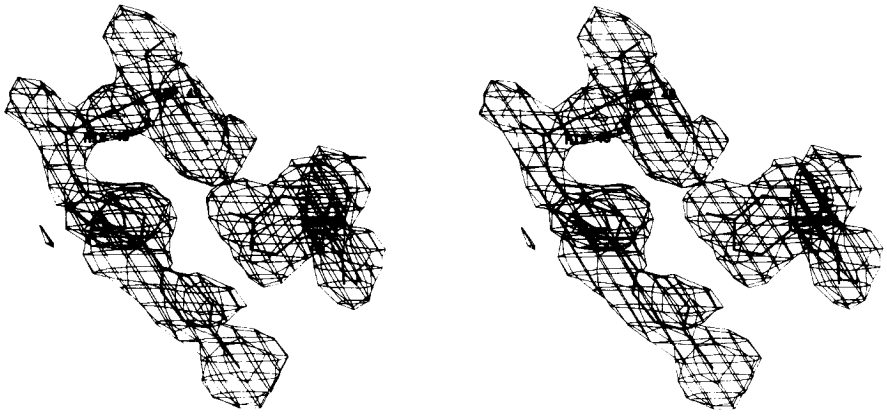

Figure 2. Stereo picture showing the electron density for the *p*-bromo-phenacyl group bound to His48 in the active site. The *p*-bromo-phenacyl group is in the lower centre of the Figure. The density for the bromine atom can be seen clearly. Also shown is the density for Tyr69 (right side of the figure).

the other interactions of the inhibitor with the enzyme are hydrophobic ones. Table 4 lists all protein atoms within 4·0 Å from each atom of the inhibitor. From Figure 3 and this Table it is clear that the active site is very easily accessible to the reagent.

While the hydrophobic part of the active site has barely changed, the conformation of the calcium binding loop (residues 28 to 33) does show obvious changes. Although at first sight the *p*-bromo-phenacyl group does not seem to interfere with the calcium binding site and enough space is available to accommodate the calcium ion, nevertheless this ion is absent. The carbonyl oxygen atoms of residues 28, 30 and 32, which were ligands to the calcium, have moved apart thereby giving a different conformation to, especially, the main-chain and side-chain atoms of Leu31. The conformation of the other calcium ligand, Asp49, has remained virtually the same. Instead of binding to calcium, this Asp side-chain makes a hydrogen bond with the hydroxyl group of Tyr69. This interaction has become possible because of an appreciable conformational change of the entire Tyr residue, by which the Tyr side-chain swings towards the active site (Fig. 4). The hydroxyl group of this side-chain has moved about 4 Å in the direction of the active site. Not only does the side-chain of this Tyr have a different conformation, also the main-chain atoms move about 1·4 Å in the direction of the active site, pulling with them residues 68, 70, 71 and 72. This results in a quite different position for Pro68. Residues 64 to 67 have a very low density, and no unambiguous position could be assigned to these residues. This is also clear from Figure 5 which shows that these residues have a very high temperature factor.

4. Discussion

We have described the structure determination of a phospholipase A_2 covalently modified at the active site histidine. Surprisingly, the conformation of the active site residues is identical with that in the native enzyme, while there are some drastic conformational differences elsewhere in the molecule. The fact that the conformation of the active site residues has not changed illustrates that the *p*-bromo-phenacyl group fits well in the active site. The inhibitor makes several hydrophobic

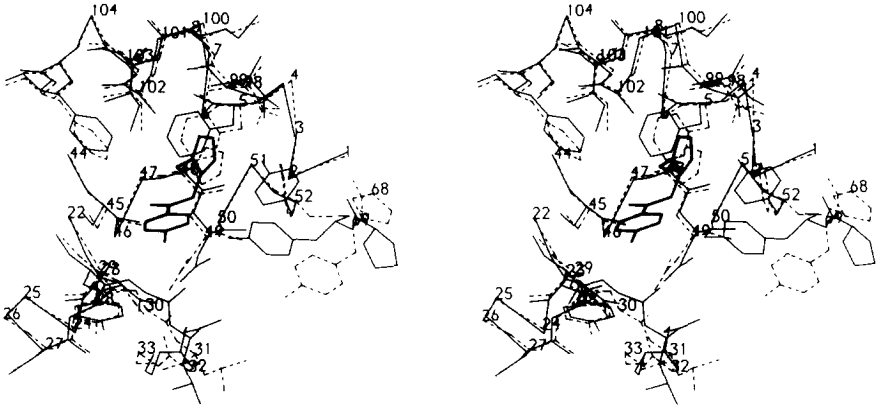

Figure 3. Stereo drawing with a comparison of the active site region in native and inhibited bovine phospholipase A_2. The native structure is represented by broken lines.

Table 4

Distances between the p-bromo-phenacyl group and protein atoms within 4·0 Å

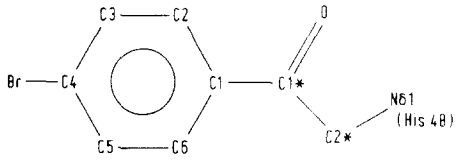

Atoms in the *p*-bromo-phenacyl moiety	Protein atom	Distance (Å)
C-2*	OH Tyr69	3·22
	CE2 Tyr52	3·46
	OD1 Asp49	3·94
C-1*	OH Tyr69	3·76
O	CA Cys45	3·36
	O Cys45	3·40
	CB Cys45	3·59
	SG Cys45	3·81
	C Cys45	3·87
C-1	OH Tyr69	3·61
	CE2 Phe5	3·67
C-2	N Gly30	3·41
C-3	N Gly30	3·10
	O Phe22	3·18
	CA Gly30	3·49
	C Cys29	3·95
C-4	CA Gly30	3·76
	N Gly30	3·89
	O Gly30	3·91
	O Phe22	3·92
C-5	OH Tyr69	3·59
	CE1 Tyr69	3·65
	CE2 Phe5	3·75
	O Gly30	3·92
	CZ Tyr69	3·98
C-6	OH Tyr69	2·88
	CE2 Phe5	3·39
	CE1 Tyr69	3·53
	CZ Tyr69	3·62
	CD2 Phe5	3·90
Br†	O Phe22	3·76
	CG Asn23	3·99
	CB Asn23	4·07
	CA Gly30	4·07
	ND2 Asn23	4·19
	CD1 Leu19	4·19
	CA Asn23	4·19
	OD1 Asn23	4·35
	C Phe22	4·35

† For the Br atom all atoms within 4·5 Å are given.

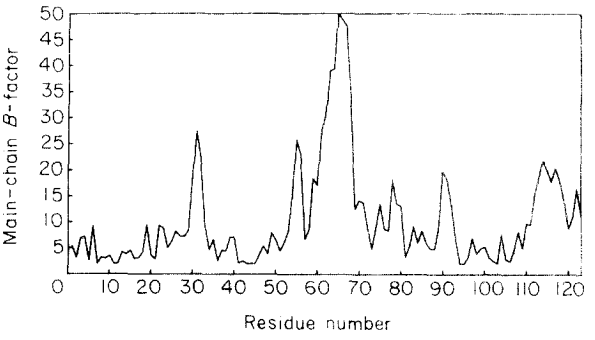

Figure 5. Average temperature factor (in Å^2) for main-chain atoms (N, C$^\alpha$, C and O) as a function of residue number.

interactions with other active site residues, and this explains why this inhibitor is rather specific for phospholipase A_2 (Volwerk *et al.*, 1974). On the other hand, the conformational differences elsewhere in the molecule seem to be mediated by the absence of calcium in the active site. Not only in the crystal, but also in solution, calcium does not bind any more to the inactivated phospholipase (Volwerk *et al.*, 1974). The reason for this observation is not very clear. Divalent cations like Ca^{2+} and Ba^{2+} have been found to protect the enzyme and pro-enzyme against inactivation by *p*-bromo-phenacyl-bromide (Volwerk *et al.*, 1974). This suggests that calcium has to leave the active site before productive binding of the inhibitor is possible. At first sight there seems to be enough room for both calcium and the inhibitor to bind in the active site. However, superposition of the native and inhibited structure shows that the position of the calcium ion and its two water ligands is such that one of these water molecules would have been within 2·6 to 2·7 Å from the aromatic ring atoms of the *p*-bromo-phenacyl group (Fig. 6). This water molecule clearly has to be removed, and this makes the binding of calcium less favourable.

From an analysis of the three-dimensional structure of native phospholipase A_2 (Dijkstra *et al.*, 1981*b*) it was proposed that the substrate binding

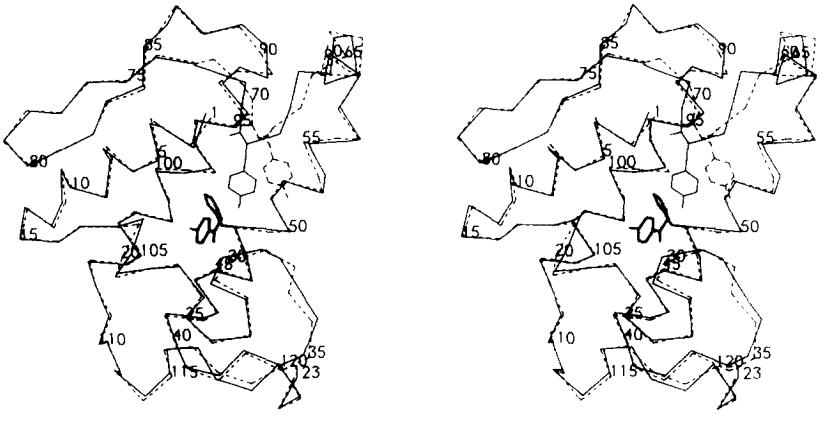

Figure 4. Stereo picture of inhibited and native phospholipase A_2, showing the conformational change of the Tyr69 residue. The native structure is indicated by broken lines.

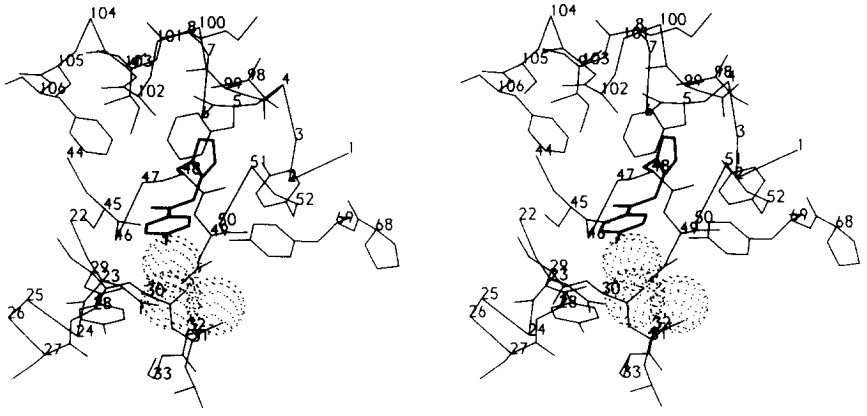

Figure 6. Stereo diagram of the *p*-bromo-phenacyl-bromide-inactivated bovine phospholipase A_2. Superimposed, in a dotted sphere representation, are the calcium ion and its 2 water ligands, in a position equivalent to that in the native structure. (In the inhibited structure no calcium ion is bound any more.) it is obvious that the contacts made by the "upper" water molecule with the aromatic ring of the covalently bound inhibitor are too short.

site consists of a hydrophobic pocket, formed by the side-chains of residues Phe5, Ile9, Phe22, Ala102, Ala103, Phe106 and the disulphide bridge between Cys29 and Cys45. Indeed, the *p*-bromo-phenacyl group binds in this hydrophobic pocket, without changing the conformation of any of these hydrophobic side-chains. This structure identifies Phe5 and Cys45 unambiguously as amino acid residues contributing to the hydrophobic binding pocket of the active centre, which we had predicted earlier. It also demonstrates the conformational freedom of the side-chain of Tyr69. At this time it is only possible to speculate on the way this residue will act in case a true substrate binds in the active site, but it is conceivable that the Tyr69 side-chain will interact with the phosphate moiety of the substrate.

Although the *p*-bromo-phenacyl group does not resemble the true substrates very much, this three-dimensional structure of the bound inhibitor might nevertheless be a good starting point for a rational design of specific and potent inhibitors. A first goal could be to improve the specificity and affinity for the phospholipase A_2 active site by adding a carbonyl group to the inhibitor, such that it could bind to calcium instead of pushing it out. Alternatively, it could be envisaged, that adding an amino group, which would sit at the calcium position and interact with Asp49 and the carbonyl oxygens in the calcium binding loop, would enhance the affinity of the inhibitor for the enzyme.

An important question remaining is the cause of the flexibility/disorder of residues 64 to 67. In the native bovine phospholipase A_2 the conformation of this 64 to 67 loop is stabilized by hydrogen bond interactions between the side-chains of Asp66 and Asn71 (H-bond distance 2·9 Å), and between the Asn67 side-chain and the O^{γ} atom of Thr70 (H-bond distance 3·3 Å). In the inhibited structure residues 68 to 72 have moved in the direction of the active site, and residues 64 to 67 have become invisible in the electron density maps. We therefore suggest that the shift of residues 70 and 71, which is about 1 to 2 Å, is too large to maintain the above-mentioned hydrogen bonds. This causes the destabilization of the conformation of the 64 to 67 loop as found in the native enzyme.

In other phospholipases A_2 conformational differences or flexibility/disorder have also been found in this part of the molecule. In porcine phospholipase the conformation of the loop from residue 63 to 72 was found to be well defined, but substantially different from that in the bovine enzyme. This different conformation has been attributed to one single amino acid substitution (Val63 to Phe63; Dijkstra *et al.*, 1983*b*). In the bovine pro-phospholipase, as well as in an N-terminally modified bovine phospholipase A_2 (Dijkstra *et al.*, 1984), an even more extensive flexibility than in the present structure has been demonstrated. In these structures the loop from residues 63 to 72 was found to be flexible, both in solution and crystal structure. Thus, this part of the molecule can easily adopt several different conformations, which apparently barely differ in energy.

In the pro-phospholipase and the N-terminally modified phospholipase A_2 the flexibility of the 63 to 72 loop has been correlated with a diminished affinity towards lipid aggregates, like micelles. In the present structure only residues 64 to 67 are not visible in the electron density maps, and are therefore disordered or flexible. Because the inhibited enzyme shows an unaltered affinity for aggregated substrates (Pieterson *et al.*, 1974*b*) residues 64 to 67 are probably not too important for the binding of lipid aggregates.

In this paper we have described the refined three-dimensional structure of covalently inhibited phospholipase A_2 from bovine pancreas. This structure has allowed us to define part of the hydrophobic binding site for monomeric substrates. It also provides us with a starting point for the continuation of our work on phospholipase A_2 towards a rational design of potent and specific inhibitors for this enzyme. In addition, we aim at the structure determination of a (non-covalent)

enzyme–inhibitor complex, in order to obtain more insight into the catalytic mechanism of phospholipase A_2.

We thank Professor G. H. de Haas and co-workers for generously supplying protein material. The stimulating discussions with Professor W. G. J. Hol are gratefully acknowledged. This work was supported by the Netherlands Foundation for Chemical Research with financial aid from the Netherlands Organization for the Advancement of Pure Research.

References

Agarwal, R. C. (1978). *Acta Crystallogr. sect. A*, **34**, 791–809.

Arndt, U. W. & Wonacott, A. J. (1977). *The Rotation Method in Crystallography*, North-Holland Publishing Company, Amsterdam.

Brandenburg, N. P., Dempsey, S., Dijkstra, B. W., Lijk, L. J. & Hol, W. G. J. (1981). *J. Appl. Crystallogr.* **14**, 274–279.

Brunie, S., Bolin, J., Gewirth, D. & Sigler, P. B. (1985). *J. Biol. Chem.* **260**, 9742–9749.

Deisenhofer, J. (1981). *Biochemistry*, **20**, 2361–2370.

Dennis, E. A. (1983). In *The Enzymes* (Boyer, P. D., ed.), 3rd edit., vol. 16, pp. 307–353, Academic Press, New York.

de Winter, J. M., Vianen, G. M. & van den Bosch, H. (1982). *Biochim. Biophys. Acta*, **712**, 332–341.

Dijkstra, B. W., Kalk, K. H., Hol, W. G. J. & Drenth, J. (1981*a*). *J. Mol. Biol.* **147**, 97–123.

Dijkstra, B. W., Drenth, J. & Kalk, K. H. (1981*b*). *Nature (London)*, **289**, 604–606.

Dijkstra, B. W., van Nes, G. J. H., Kalk, K. H., Brandenburg, N. P., Hol, W. G. J. & Drenth, J. (1982). *Acta Crystallogr. sect. B*, **38**, 793–799.

Dijkstra, B. W., Renetseder, R., Kalk, K. H., Hol, W. G. J. & Drenth, J. (1983*a*). *J. Mol. Biol.* **168**, 163–179.

Dijkstra, B. W., Weijer, W. J. & Wierenga, R. K. (1983*b*). *FEBS Letters*, **164**, 25–27.

Dijkstra, B. W., Kalk, K. H., Drenth, J., de Haas, G. H., Egmond, M. R. & Slotboom, A. J. (1984). *Biochemistry*, **23**, 2759–2766.

Dodson, E. J., Isaacs, N. W. & Rollett, J. S. (1976). *Acta Crystallogr. sect. A*, **32**, 311–315.

Forst, S., Weiss, J., Elsbach, P., Maraganore, J. M., Reardon, I. & Heinrikson, R. L. (1986). *Biochemistry*, **25**, 8381–8385.

Halpert, J., Eaker, D. & Karlsson, E. (1976). *FEBS Letters*, **61**, 72–76.

Hamilton, W. C., Rollett, J. S. & Sparks, R. A. (1965). *Acta Crystallogr.* **18**, 129–130.

Hendrickson, W. A. (1985). *Methods Enzymol.* **115B**, 252–270.

Kabsch, W. (1976). *Acta Crystallogr. sect. A*, **32**, 922–923.

Lewis, R. A. & Austen, K. F. (1981). *Nature (London)*, **293**, 103–108.

Pieterson, W. A., Volwerk, J. J. & de Haas, G. H. (1974*a*). *Biochemistry*, **13**, 1439–1445.

Pieterson, W. A., Vidal, J. C., Volwerk, J. J. & de Haas, G. H. (1974*b*). *Biochemistry*, **13**, 1455–1460.

Rao, S. T. & Rossmann, M. G. (1973). *J. Mol. Biol.* **76**, 241–256.

Read, R. J. (1986). *Acta Crystallogr. sect. A*, **42**, 140–149.

Renetseder, R., Brunie, S., Dijkstra, B. W., Drenth, J. & Sigler, P. B. (1985). *J. Biol. Chem.* **260**, 11627–11634.

Schwager, P., Bartels, K. & Huber, R. (1973). *Acta Crystallogr. sect. A*, **29**, 291–295.

Sim, G. A. (1959). *Acta Crystallogr.* **12**, 813–815.

Sim, G. A. (1960). *Acta Crystallogr.* **13**, 511–512.

Stewart, J. M. (1976). *The XRAY-system*, Technical Report TR-446 of the Computer Science Center, University of Maryland, College Park, MD (U.S.A.).

van den Bosch, H. (1980). *Biochim. Biophys. Acta*, **604**, 191–246.

Verheij, H. M., Slotboom, A. J. & de Haas, G. H. (1981). *Rev. Physiol. Biochem. Pharmacol.* **91**, 91–203.

Volwerk, J. J. & de Haas, G. H. (1982). In *Lipid–Protein Interactions* (Jost, P. C. & Griffith, O. H., eds), pp. 69–149, Wiley, New York.

Volwerk, J. J., Pieterson, W. A. & de Haas, G. H. (1974). *Biochemistry*, **13**, 1446–1454.

Wells, M. A. (1973). *Biochemistry*, **12**, 1080–1085.

Edited by R. Huber